JACS
JOURNAL OF THE AMERICAN CHEMICAL SOCIETY
Article
pubs.acs.org/JACS

Capillary Bridging as a Tool for Assembling Discrete Clusters of Patchy Particles

Bhuvnesh Bharti,*[,†,‡] David Rutkowski,[†] Koohee Han,[†] Aakash Umesh Kumar,[†] Carol K. Hall,[†] and Orlin D. Velev*[,†]

[†]Department of Chemical and Biomolecular Engineering, North Carolina State University, Raleigh, North Carolina 27695, United States

[‡]Cain Department of Chemical Engineering, Louisiana State University, Baton Rouge, Louisiana 70803, United States

Supporting Information

ABSTRACT: Janus and patchy particles are emerging as models for studying complex directed assembly patterns and as precursors of new structured materials and composites. Here we show how lipid-induced capillary bridging could serve as a new and nonconventional method of assembling patchy particles into ordered structures. Iron oxide surface patches on latex microspheres were selectively wetted with liquid lipid, driving the particle assembly into two- and three-dimensional clusters via interparticle capillary bridge formation. The liquid phase of the bridges allows local reorganization of the particles within the clusters and assists in forming *true* equilibrium configurations. The temperature-driven fluid-to-gel and gel-to-fluid phase transitions of the fatty acids within the bridge act as a thermal switch for cluster assembly and disassembly. By complementing the experiments with Monte Carlo simulations, we show that the equilibrium cluster morphology is determined by the patch characteristics, namely, their size, number, and shape. This study demonstrates the ability of capillary bridging as a versatile tool to assemble thermoresponsive clusters and aggregates. This method of binding particles is simple, robust, and generic and can be extended further to assemble particles with nonspherical shapes and complex surface chemistries enabling the formation of sophisticated colloidal molecules.

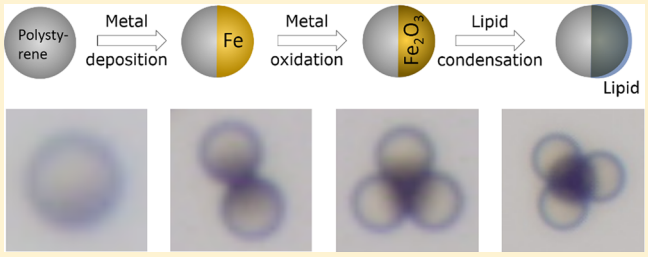

1. INTRODUCTION

Self-assembly of atoms, molecules, and particles is the origin of all physical mesoscopic matter.[1,2] The properties of these materials are governed by the spatial organization and symmetry of the particle assemblies. The equilibrium morphology of the self-assembled state of these building blocks is determined by their packing efficiency (entropy) and interparticle interaction (enthalpy), but the lack of means of controlling these parameters hinders the fabrication of structures with complex functionality. In order to further extend the role of self-assembly, colloidal particles with directional pair interactions have been proposed as precursors to generate ordered domains and clusters with unusual patterns and symmetry.[3−7] The key parameters determining the assembled state of these particles are the number of surface interaction sites (patches), the surface patch area, the magnitude of the interaction potential, the packing efficiency, and the particle shape.[2,8−13] The interparticle interactions play a major role in driving and governing the assembly process. To assemble ordered domains and structures, these interactions must allow particle-to-particle reorganization in order to inhibit the occurrence of kinetically trapped configurations and attain a thermodynamic minimum-energy state.

The binding forces used in colloidal self-assembly include electrostatic and van der Waals (DLVO type), hydrophobic, and lock-and-key type (DNA and other molecular-recognition binding) interactions.[14−19] One nonconventional method of binding particles is through the formation of capillary bridges. In this case, particles wetted with a liquid that come into surface contact with each other attain an interconnected state, where the wetting liquid forms interparticle capillary bridges.[20−23] The origin of capillary attraction is the interfacial tension between the dispersing liquid and the surface-wetting liquid. This is in contrast to the molecular mechanism of hydrophobic attraction, where the entropy gain due to loss of water molecules during the binding process is the driving force. The capillary forces are spatially isotropic and, much like oppositely charged particle pairs, yield random aggregates.[20,24] A directional aspect to the interactions can be introduced by spatially defining the interaction spots on a particle's surface, i.e., discretizing the interaction domain and hence introducing spatial restriction in the interactions.[25] For example, silica/gold Janus particles in water/2,6-lutidine binary liquid mixtures exhibit temperature-controlled wetting of the particles.[26] In the two-phase region of the binary liquid, water preferentially wets the silica hemisphere, resulting in the formation of capillary-bridged two-dimensional (2D) clusters. These self-assemblies exist within a

Received: August 3, 2016
Published: October 24, 2016

DOI: 10.1021/jacs.6b08017
J. Am. Chem. Soc. 2016, 138, 14948−14953

narrow temperature range of 1−2 °C.[26] Beyond this temperature range, macroscopic phase separation of the two liquids occurs, resulting in the formation of particle-covered Pickering emulsion droplets.[27,28]

In this article we present an approach for liquid-lipid-based capillary binding of patchy particles into colloidal clusters over a wide temperature range without macroscopic phase separation or emulsion formation. The capillary binding enables completely reversible assembly and disassembly of clusters during capillary bridge freezing and melting cycles. Both experimentally and by using Monte Carlo simulations, we show that the near-equilibrium morphology of the colloidal clusters is governed by the physical properties of the surface patches on the particles.

We induce direct condensation of the surface-wetting agent (lipid) from the bulk onto the surface patch of a microparticle to create interaction sites. This approach stems from our recent report on the assembly of iron oxide nanoparticles into networked filaments via capillarity-mediated binding between liquid-lipid shells on the particles.[22] The strong affinity of the fatty acids for iron oxide[29] leads to surface wetting and formation of a condensed liquid-lipid shell selectively on the patch. The spatial overlap of these liquid shells on the patches leads to the formation of capillary bridges between the iron oxide nanoparticles.[30]

2. RESULTS AND DISCUSSION

This report is based on the use of 4 μm latex microspheres with iron oxide surface patches as building blocks for assembling 2D and 3D clusters. The surface patches were formed on negatively charged polystyrene microbeads by the previously reported technique of metal (here iron) vapor deposition.[31] The iron patch size, shape, and orientation were fine-tuned by changing the angle of the deposition. Here we define the fractional patch area (f) as a measure of the particle's patchiness (or Janus balance). The value of f was determined by analyzing scanning electron microscopy (SEM) images (Figure S1), where $f = a_{patch}/a_{total}$, in which a_{patch} and a_{total} are the iron patch area and the total surface area of the particle, respectively. In order to minimize residual magnetization and van der Waals attraction, the layer of iron metal deposited on the particles was only 5 nm thick.[32] It has previously been shown that upon transfer of the iron-patched particles into an aqueous dispersion, a layer of iron oxide spontaneously forms on the patch.[33] Subsequent addition of fatty acid amine salts at pH 9.5 results in selective wetting of the iron oxide patch with a liquid-lipid layer, which promotes the formation of interparticle capillary bridges (Scheme 1a).

The self-assembly of patchy colloids is governed by the surface interaction between the particles. In our case of metallo−dielectric patchy particles, we determined the surface potential of the sulfonate-functionalized polymer hemisphere by measuring the electrophoretic mobility of unpatched polystyrene microbeads. The surface potential for the metal patch at pH 9.5 was determined by measuring the zeta potential of an iron oxide-coated flat substrate using tracer particles (for measurement details, see Figure S2). The surface potentials were measured both in water and in fatty acid salt solution. The net zeta potentials of all of the surfaces were found to be in the range from −20 to −50 mV, and hence, the surfaces were electrostatically repulsive (Figure S3 and Scheme 1b).

2.1. Liquid-Lipid-Driven Particle Clustering. In a typical experiment, patchy microspheres were dispersed in aqueous fatty acid amine salt solution and transferred into a sealed microchamber. The particles were allowed to self-assemble at a preset temperature, and the kinetics of the assembly process was monitored using an Olympus BX-61 microscope. Initially, only single particles or low-aggregation-number clusters were observed. At a fixed particle concentration, the mean cluster-aggregation number increases over time because of the increasing probability of patch-to-patch encounters, resulting in capillary-bridged clusters (Figure S4). The gravitational force acting on the particles restricted the colloidal clusters to the bottom of the assembly chamber. The near-equilibrium structures formed (after 9 h) by the lipid-wetted Janus particles (f = 0.5) are shown in Figure 1. The micrograph shows the coexistence of 2D planar and 3D structures. We investigated the specific case of low particle number density (<2 vol %), where discrete clusters were formed and no network or lattice formation was observed.

The capillary interaction driving microparticle cluster formation is unique in several fundamental aspects. When the lipid-wetted surface patches approach each other, there is an initial electrostatic repulsion followed by a short-range square-well-like attraction at even closer separations (Scheme 1b).[30,34] This attraction has been attributed to the formation of capillary bridging between the liquid-coated particles/patches.[30,35] In the present case of lipid-wetted particles, the capillary bridging dominates other secondary interactions (van der Waals, electrostatic, etc.) and drives the self-assembly process. The capillary binding forces are known to be orders of magnitude stronger than other conventional forces (electrostatic, van der Waals, etc.).[36] Despite the strong attraction, we observed that the liquid nature of the bridges allows high reconfigurability of the interparticle "bonds". In our experiments, we commonly see

Scheme 1. (a) Schematic Summarizing the General Methodology for Fabricating Lipid-Patched Polystyrene (PS) Microspheres; (B) Interactions between All Three Surface Pairs of the Patchy Microparticle[a]

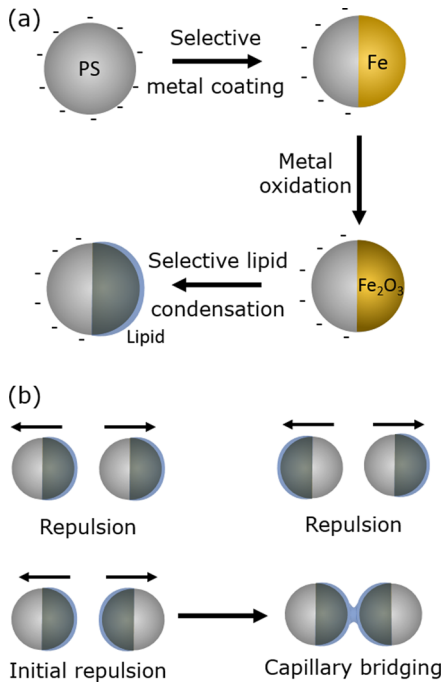

[a]Here the thickness of the liquid fatty acid layer and the particle size are not drawn to scale.

DOI: 10.1021/jacs.6b08017
J. Am. Chem. Soc. 2016, 138, 14948−14953

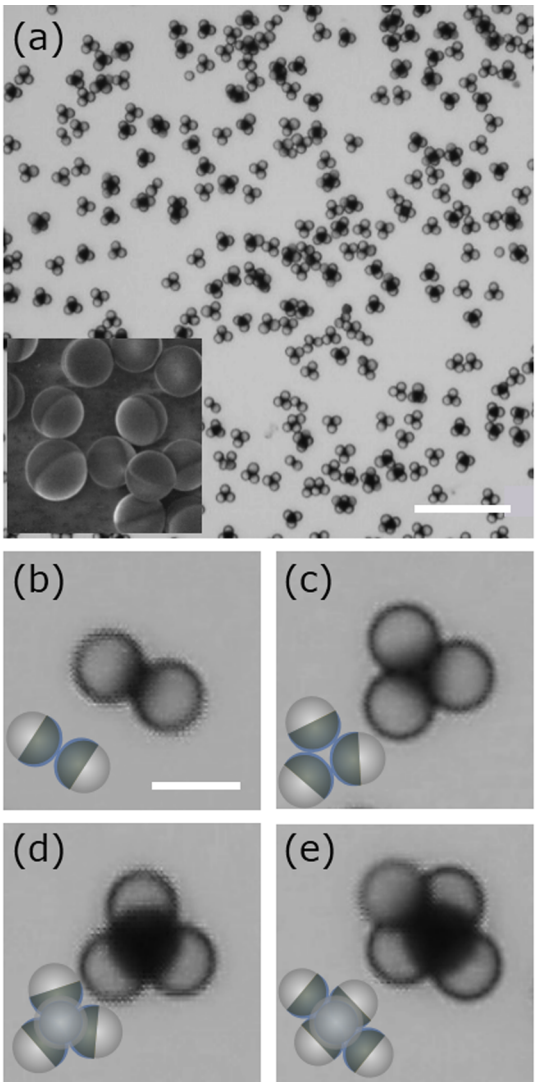

Figure 1. (a) Optical micrographs illustrating the self-assembly of lipid-wetted Janus particles into ordered colloidal clusters in aqueous dispersion. The inset shows an SEM image of the Janus particles before assembly in the dried state. (b–e) Examples of 2D and 3D clusters formed by capillary binding of the microspheres. The scale bars are (a) 50 μm and (b) 5 μm.

that when two independent clusters coalesce, the individual particles within the parent cluster reorient to accommodate the changed aggregation number (movie 1). The ability of liquid bridges to realign the bound particles is the key to attain true equilibrium morphology of the clusters. Here the local stresses within a kinetically trapped cluster are dissipated by particle-to-particle rollover and reorientation, allowing a minimum-energy state to be achieved. This assembly/reassembly of patchy particles is different from the self-assembly driven by strong hydrophobic, electrostatic, or van der Waals interactions, where such reconfigurations are not expected.[37,38] A decrease in the magnitude of the net interparticle interaction (~thermal energy) also results in structural reconfigurability.[39] In the present case of strong capillary binding (much larger than the thermal energy),[22] the reorientation of the linked particles is solely due to liquid fatty acid.

2.2. Thermal Switching of Clusters. Fatty acid aqueous dispersions have the ability to spontaneously transition between fluid and gel phases. The corresponding phase transition temperature (T_P) depends upon the number of carbon atoms in the fatty acid backbone and the identity of the dispersing counterion.[22] The effect of the fatty acid phase change on the self-assembly of Janus particles was investigated using ethanolamine salts of dodecanoic acid ($C_{11}H_{23}COOH$, $T_P \approx 8$ °C) and hexadecanoic acid ($C_{15}H_{31}COOH$, $T_P \approx 40$ °C).[22] The data for the temperature dependence of the fraction of particles assembled (nonsinglet particles) in $C_{11}H_{23}COOH$ and $C_{15}H_{31}COOH$ are shown in Figure 2a. For $C_{11}H_{23}COOH$,

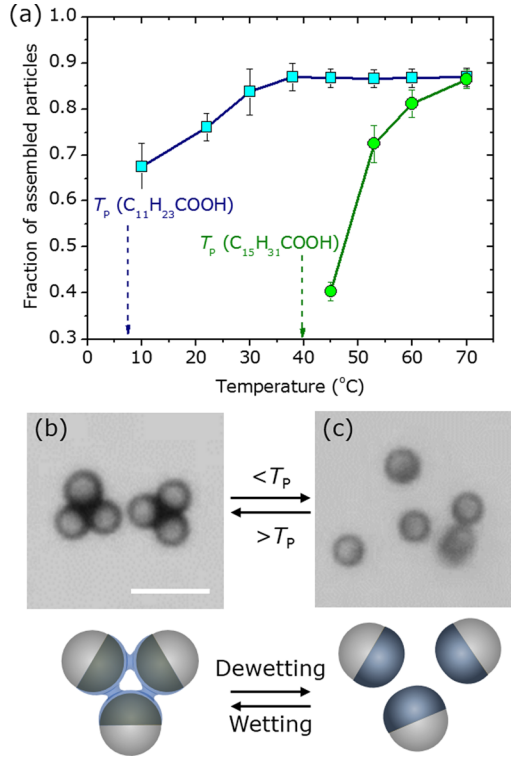

Figure 2. (a) Fractions of Janus particles self-assembled into clusters at different temperatures for ethanolamine salts of *n*-dodecanoic acid (squares) and *n*-hexadecanoic acid (circles). The vertical lines indicate the fluid-to-gel phase transition temperatures (T_P) of the fatty acids on iron oxide surfaces. (b, c) The clusters disassemble when the temperature is decreased to below the fluid-to-gel phase transition temperature of the fatty acid, i.e., when the liquid in the capillary bridge freezes (movie 2). At temperatures $T < T_P$, the fraction of assembled particles remains negligibly small. The corresponding schematics illustrate thermally reversible capillary bridge formation and rupturing. The scale bar in (b) is 10 μm.

the Janus particles spontaneously assembled into clusters below 40 °C, whereas no assembly was observed for $C_{15}H_{31}COOH$ in this temperature range. In the case of $C_{15}H_{23}COOH$, the assembly was observed only above the corresponding phase transition temperature (40 °C). This observation indicates that the fluidity of the fatty acid is a prerequisite for the assembly process. We believe that a lipid surface patch is "sticky" only when the adsorbed lipid layer is in the fluid state, which further leads to capillary bridging and particle assembly. The gel-to-fluid and fluid-to-gel transformation of lipids is a first-order phase transition, and hence, the particles can be thermally triggered to adopt either a fully assembled or disassembled state (Figure 2a).

The observed dependence of the capillary bridge formation on the lipid phase transition leads to an intriguing question of

DOI: 10.1021/jacs.6b08017
J. Am. Chem. Soc. 2016, 138, 14948–14953

what happens to a cluster when the capillary bridges "freeze". This was investigated for clusters formed by $C_{15}H_{23}COOH$ at 50 °C ($>T_P$) by gradually lowering the temperature to 30 °C. We found that the preassembled clusters disintegrated when the temperature was decreased to below the corresponding phase transition temperature (movie 2 and Figure 2b,c). The cooling results in lipid gelation, making the interparticle capillary bridges brittle, which causes their subsequent fracture.[22] The lipid gelation might also result in effective dewetting of the surface patch and the observed disassembly. Further studies would provide a complete understanding of the impact of the lipid phase behavior on the patch and on the capillary bridging.

2.3. Monte Carlo Simulations of Patchy Particle Clustering. The interparticle interactions involved in the capillary bridging and cluster formation could be affected in a nontrivial way by several control parameters, and hence, a concurrent theoretical/simulation approach is necessary to better understand the process. We developed a simple Monte Carlo (MC) simulation model to interpret our experimental observations. Similar models have been used previously to predict the self-assembly of Janus particles.[40] Each individual particle was modeled by a set of 252 evenly spaced domains covering the surface of a central spherical core.[41] On the basis of our experimental findings (Scheme 1b), the surface domains on the particle were divided into two types representing (1) charged polymer surface (type A) or (2) lipid-coated surface patch (type B). The two types of domains cover a central core such that the resulting particle contains a single patch of type B with fractional surface coverage f (Figure 3a inset). In the MC simulations, the fractional patch area was defined to be the fraction of A domains on a particle. The capillary bridging attractive interaction between B domains was approximated by a short-range attractive square-well potential with a well width of 0.3σ, where σ is the diameter of the patchy particle, and a well depth of 1.0ε, where ε is the interaction energy in arbitrary units. The corresponding minimum energy between a pair of colloidal particles varied between 270ε and 590ε depending on the value of f. The simulations were performed at $T^* = kT/\varepsilon = 32.9$, which corresponds to a real temperature of 298 K. The $A-A$ and $A-B$ interactions were modeled by square shoulders of the same width and magnitude as the square well describing the $B-B$ interactions. The overall interaction between such patchy spheres was the sum of the $A-A$, $A-B$, and $B-B$ interactions. In a typical simulation run, 100 particles were randomly placed in a cubic simulation box with an edge length of approximately 28σ. The simulations were performed with periodic boundary conditions in the x and y directions and a hard-wall boundary in the z direction. In our experiments, the gravitational force restricts the clusters to the bottom of the assembly chamber. To account for this effect in our simulations, we introduced an additional gravitational potential acting on the particle clusters in the z direction of the simulation box. Because of this quasi-2D character of our system, we specify the particle area fraction for the xy plane projections of the Janus spheres (instead of the spheres' total volume fraction) and set it to 0.10. The near-equilibrium assemblies were formed in our simulations by minimizing the ensemble energy (movie 3). Further details on the simulation procedure are provided in the Supporting Information.

The assemblies formed by patchy particles (with $f = 0.15$) in our MC simulations and experiments are shown in Figure 3a,b, respectively. Both the simulations and experiments show the

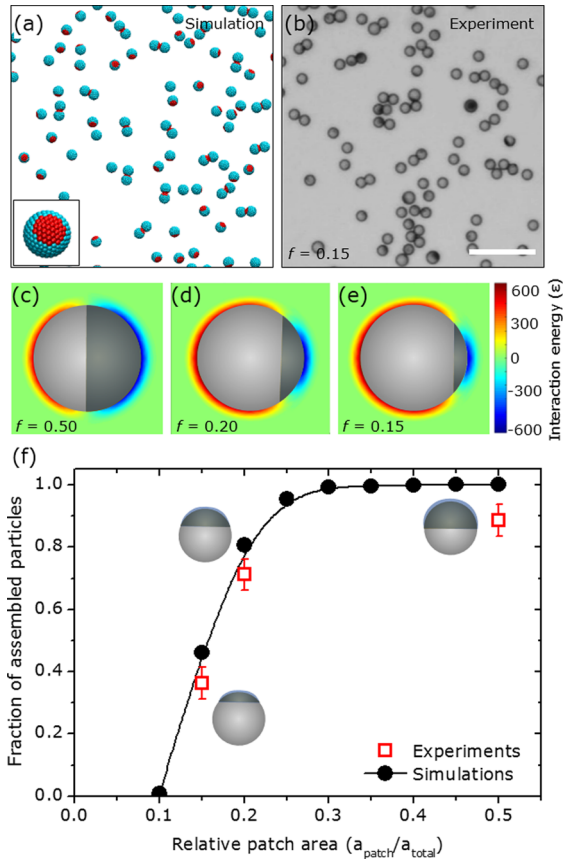

Figure 3. (a) Self-assemblies formed by the patchy particles ($f = 0.15$) in Monte Carlo simulations of the capillary assembly process. The inset shows an individual particle unit formed by distributing 252 domains on a central core. (b) Micrograph of patchy microspheres with fractional patch area of 0.15 assembled into low-aggregation-number clusters. (c–e) Surface interaction energy map for particles with different patch sizes (f = 0.50, 0.20, and 0.15). The attractive interaction between the lipid-coated patches was modeled on the basis of a square-well attractive potential. (f) Increase in the fraction of assembled particles with increasing relative patch area (f) in simulations (solid circles) and experiments (open squares). The scale bar in (b) is 50 μm.

presence of low-aggregation-number 2D clusters. Here we investigate the change in the cluster morphology with increasing patch area. In our MC simulation, the surface patch area can be increased by increasing the relative population of B domains on a particle (Figure 3c–e), whereas in experiments it can be increased by changing the relative angle of metal vapor deposition onto the particles.[31] In both the experiments and MC simulations, we find an increase in the fraction of particles assembled with increasing surface patch area; the experimental observations (Figure 3f, open squares) overlay the MC simulation findings (Figure 3f, solid circles, and Figure S5). In addition, we find that the simulated assembly kinetics of particles with different patch sizes is qualitatively similar to that in our experiments (Figure S6). The simulations offer a facile fundamental tool to determine the clustering pathways followed by particles with different patch characteristics and to understand why specific cluster morphologies arise under different physical conditions. They help guide the design of colloidal building blocks that will self-assemble into clusters of unusual morphology, which is nontrivial to establish by experiments alone. The simulations also show that the

DOI: 10.1021/jacs.6b08017
J. Am. Chem. Soc. 2016, 138, 14948–14953

interactions among the experimental particles can be approximated reasonably well by a patchy sphere model with simple short-range interactions. Because the simulations describe the experimental assembly quite well, they could be used to explore patch configurations that have not yet been fabricated.

2.4. Capillary Bridging of Complex Particles and Their Mixtures. The potential of the method to achieve complexity in the interactions and the assembled cluster morphologies can be illustrated by using multidisperse building block particles or by changing the patch morphology. A few representative clusters formed by a mixture of 4 and 2 μm Janus particles are shown in Figure 4a–c. The particles assembled into mixed

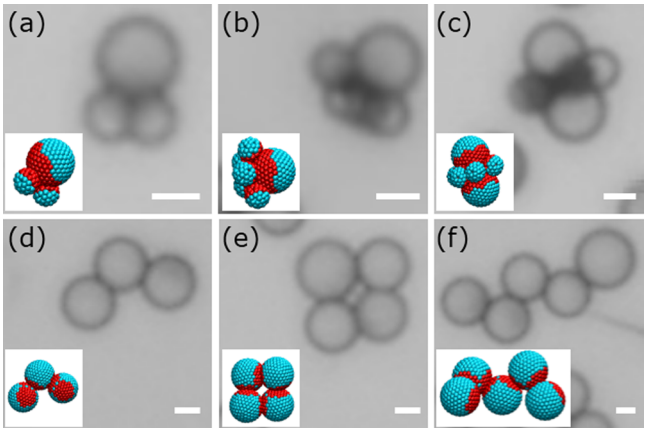

Figure 4. (a–c) Micrographs of the assemblies formed by a mixture of 4 and 2 μm Janus particles. (d–f) Capillary-bridged self-assemblies formed by double-patched microspheres. The insets in the frames are the clusters observed in corresponding Monte Carlo simulations. The scale bar in each image is 2 μm.

clusters composed of both small (diameter ~2 μm) and large (diameter ~4 μm) Janus particles. A wide variety of self-assembled structures were observed, including biparticle dimers and trimers (Figure 4a), a hexamer with one large and five small particles (Figure 4b), and small-particle rings around large particle dimers (Figure 4c). We believe that the morphology of the assembled clusters is determined by the minimization of the net balance of the repulsive electrostatic and attractive capillary interactions on a particle within the clusters. The range and absolute magnitude of the interactions play a key role in guiding the self-assembly process and the near-equilibrium structures. The capillary bridging allows local reorganization of the bound particles and hence favors the maximization of patch-to-patch contact area within a cluster (Figure S7). This reorganization of particles stems from minimization of the capillary binding energy by immediate rearrangement of the interparticle bridges. This is in contrast to the case of strong electrostatic and other conventional forces that bind the particles into clusters, where such rearrangements and corresponding assemblies are rarely observed.[38] Here again, our MC simulations correctly predict the assembly of the complex structures in the experiments (Figure 4a–c insets).

The shape and number of "sticky patches" on a particle surface greatly influence the equilibrium morphology of self-assembled clusters. We illustrated this by introducing two distinct iron oxide patches onto the 4 μm particles by selective metal vapor deposition. Unlike previous studies where the patches were located diagonally opposite each other on the surface of particles,[42] the triangular patches were introduced adjacent to each other (SEM, Figure S1). Experimental images of clusters formed by these double-patched particles are shown in Figure 4d–f. Here the self-assemblies formed both in experiment and in MC simulations (Figures 4d–f and S7b) were limited to two dimensions, with spatially loose or open clusters. The formation of 2D clusters by the double-patched particles can be attributed to the low surface fraction patch area, which restricts the formation of 3D assemblies. The two discrete patches on the surface induce an additional directionality in the assembly process that favors the formation of elongated assemblies, reminiscent of copolymerization (Figures 4f and S7).[43] Many more types of multipatchy assemblies can be realized by capillary binding of engineered particles with complex shapes and surface patch characteristics. Liquid bridging facilitates new pathways to self-assemble micro- and nanoscale building blocks into clusters with unusual symmetries and morphologies.

3. CONCLUSIONS

We have found that the thermoresponsive self-assembly of microparticles can be directed by selective surface wetting and formation of capillary bridges between the patches on the particles. Wetting of the patches induces a short-range attractive potential that guides the assembly of particles into clusters of desired morphologies. Minimization of the capillary binding energy by spatial reconfiguration of the flexible bridges drives the cluster reassembly and growth. We believe that the reconfigurability of particles linked via capillary bridges will assist in assembling equilibrium states of faceted particles, which otherwise are restricted to dissipate local stresses because of the anisotropic shape and non-reconfigurable interparticle binding. The liquid characteristic of capillary-bridging-driven assembly may also result over time in defect-free colloidal clusters and lattices. In other words, the initial defects can be self-repaired by particle reorganization enabled by the liquid-based capillary binding. We believe that this method of liquid-lipid bridging opens up new opportunities to assemble clusters, networks, and lattices of anisotropic colloidal building blocks with unusual physical, chemical, and optical properties.

■ ASSOCIATED CONTENT

Supporting Information

The Supporting Information is available free of charge on the ACS Publications website at DOI: 10.1021/jacs.6b08017.

Technical details of the simulation procedure, surface charge characterization, SEM images of the patchy microparticles, and kinetics of the self-assembly process followed by experiments and Monte Carlo simulations (PDF)

Movie showing patch-to-patch capillary binding of Janus particles (AVI)

Movie showing temperature-induced colloidal cluster disintegration (AVI)

Movie showing a Monte Carlo simulation of Janus particle self-assembly (AVI)

■ AUTHOR INFORMATION

Corresponding Authors

*bbharti@lsu.edu

*odvelev@ncsu.edu

DOI: 10.1021/jacs.6b08017
J. Am. Chem. Soc. 2016, 138, 14948–14953

Notes

The authors declare no competing financial interest.

■ ACKNOWLEDGMENTS

The financial support by the NSF grant CBET-1604116 and by the Research Triangle MRSEC on Programmable Soft Matter, DMR-1121107, is gratefully acknowledged. We thank Sangchul Roh for assistance with SEM measurements.

■ REFERENCES

(1) Whitesides, G. M.; Grzybowski, B. *Science* **2002**, *295*, 2418.
(2) Zhang, J.; Luijten, E.; Granick, S. *Annu. Rev. Phys. Chem.* **2015**, *66*, 581.
(3) Walther, A.; Müller, A. H. E. *Chem. Rev.* **2013**, *113*, 5194.
(4) Sacanna, S.; Rossi, L.; Pine, D. J. *J. Am. Chem. Soc.* **2012**, *134*, 6112.
(5) Zhang; Glotzer, S. C. *Nano Lett.* **2004**, *4*, 1407.
(6) Chen, Q.; Bae, S. C.; Granick, S. *J. Am. Chem. Soc.* **2012**, *134*, 11080.
(7) Bharti, B.; Velev, O. D. *Langmuir* **2015**, *31*, 7897.
(8) Chen, Q.; Yan, J.; Zhang, J.; Bae, S. C.; Granick, S. *Langmuir* **2012**, *28*, 13555.
(9) Sun, Y.; Chen, M.; Zhou, S.; Hu, J.; Wu, L. *ACS Nano* **2015**, *9*, 12513.
(10) Lenis, J.; Razavi, S.; Cao, K. D.; Lin, B.; Lee, K. Y. C.; Tu, R. S.; Kretzschmar, I. *J. Am. Chem. Soc.* **2015**, *137*, 15370.
(11) Cavallaro, M.; Botto, L.; Lewandowski, E. P.; Wang, M.; Stebe, K. J. *Proc. Natl. Acad. Sci. U. S. A.* **2011**, *108*, 20923.
(12) Botto, L.; Lewandowski, E. P.; Cavallaro, M.; Stebe, K. J. *Soft Matter* **2012**, *8*, 9957.
(13) Lewandowski, E. P.; Cavallaro, M.; Botto, L.; Bernate, J. C.; Garbin, V.; Stebe, K. J. *Langmuir* **2010**, *26*, 15142.
(14) Zhou, Y.; Wang, D.; Huang, S.; Auernhammer, G.; He, Y.; Butt, H.-J.; Wu, S. *Chem. Commun.* **2015**, *51*, 2725.
(15) Wang, Y.; Wang, Y.; Zheng, X.; Ducrot, É.; Yodh, J. S.; Weck, M.; Pine, D. J. *Nat. Commun.* **2015**, *6*, 7253.
(16) McGinley, J. T.; Jenkins, I.; Sinno, T.; Crocker, J. C. *Soft Matter* **2013**, *9*, 9119.
(17) Rogers, W. B.; Manoharan, V. N. *Science* **2015**, *347*, 639.
(18) Jones, M. R.; Seeman, N. C.; Mirkin, C. A. *Science* **2015**, *347*, 1260901.
(19) Chen, Q.; Whitmer, J. K.; Jiang, S.; Bae, S. C.; Luijten, E.; Granick, S. *Science* **2011**, *331*, 199.
(20) Koos, E.; Willenbacher, N. *Science* **2011**, *331*, 897.
(21) Butt, H.-J.; Kappl, M. *Adv. Colloid Interface Sci.* **2009**, *146*, 48.
(22) Bharti, B.; Fameau, A.-L.; Rubinstein, M.; Velev, O. D. *Nat. Mater.* **2015**, *14*, 1104.
(23) Bowden, N.; Choi, I. S.; Grzybowski, B. A.; Whitesides, G. M. *J. Am. Chem. Soc.* **1999**, *121*, 5373.
(24) Bharti, B.; Findenegg, G. H.; Velev, O. D. *Sci. Rep.* **2012**, *2*, 1004.
(25) Lipowsky, R. *Curr. Opin. Colloid Interface Sci.* **2001**, *6*, 40.
(26) Yu, C.; Zhang, J.; Granick, S. *Angew. Chem., Int. Ed.* **2014**, *53*, 4364.
(27) Velev, O. D.; Furusawa, K.; Nagayama, K. *Langmuir* **1996**, *12*, 2374.
(28) Dinsmore, a D.; Hsu, M. F.; Nikolaides, M. G.; Marquez, M.; Bausch, A. R.; Weitz, D. A. *Science* **2002**, *298*, 1006.
(29) Chernyshova, I. V.; Ponnurangam, S.; Somasundaran, P. *Langmuir* **2011**, *27*, 10007.
(30) Bharti, B.; Fameau, A.-L.; Velev, O. D. *Faraday Discuss.* **2015**, *181*, 437.
(31) Pawar, A. B.; Kretzschmar, I. *Macromol. Rapid Commun.* **2010**, *31*, 150.
(32) Shemi, O.; Solomon, M. J. *Langmuir* **2014**, *30*, 15408.
(33) Ren, B.; Ruditskiy, A.; Song, J. H. K.; Kretzschmar, I. *Langmuir* **2012**, *28*, 1149.
(34) Zemb, T.; Kunz, W. *Curr. Opin. Colloid Interface Sci.* **2016**, *22*, 113.
(35) Hijnen, N.; Clegg, P. S. *Langmuir* **2014**, *30*, 5763.
(36) Min, Y.; Akbulut, M.; Kristiansen, K.; Golan, Y.; Israelachvili, J. *Nat. Mater.* **2008**, *7*, 527.
(37) Chandler, D. *Nature* **2005**, *437*, 640.
(38) Wang, H.; Hansen, M. B.; Löwik, D. W. P. M.; van Hest, J. C. M.; Li, Y.; Jansen, J. A.; Leeuwenburgh, S. C. G. *Adv. Mater.* **2011**, *23*, H119.
(39) Walker, D. A.; Browne, K. P.; Kowalczyk, B.; Grzybowski, B. A. *Angew. Chem., Int. Ed.* **2010**, *49*, 6760.
(40) Hong, L.; Cacciuto, A.; Luijten, E.; Granick, S. *Nano Lett.* **2006**, *6*, 2510.
(41) Hardin, R. H.; Sloane, N. J. A.; Smith, W. D. Tables of Spherical Codes with Icosahedral Symmetry. http://neilsloane.com/icosahedral.codes/ (accessed Aug 3, 2016).
(42) Mao, X.; Chen, Q.; Granick, S. *Nat. Mater.* **2013**, *12*, 217.
(43) Liu, K.; Nie, Z.; Zhao, N.; Li, W.; Rubinstein, M.; Kumacheva, E. *Science* **2010**, *329*, 197.

DOI: 10.1021/jacs.6b08017
J. Am. Chem. Soc. 2016, 138, 14948−14953